Synthesis, Characterization, Antimicrobial Activity and DNA cleavage of Transition Metal Complexes of Pyrrole-2-Carboxaldehyde with Glutamic acid

R.SUBARANI[1], P.METILDA[2]*

[1]Reg.no 12096 Research Scholar, Department of Chemistry and Research, N.M.Christian college, Marthandam, Affiliated to Manonmanium Sundranar University, Thirunelveli, Tamilnadu-629165, India.

[2*]Department of Chemistry and Research , N.M.Christian College, Marthandam,

ABSTRACT: The Schiff base ligand was prepared by condensation of pyrrole-2-carboxaldehyde with Glutamic acid. Cu(II), Co(II), Mn(II), Zn(II) and Ni(II) complexes of above ligand was synthesised as well. The synthesised ligand and complexes have characterized by IR, UV, ^{1}HNMR, EPR, Powder XRD, SEM and EDAX. The antimicrobial activity of the synthesized ligand and its complexes have been tested for their antibacterial activity against bacterial species Basillus subtilis, Bacillus cereus, Escherichia coli, Klebsiella pneumoniae, Pseudomonaos aeruginosa, Staphylococcus aureus and fungal species Candida albicans and Aspergillus niger. The result found that the metal complexes were more active than the ligand. Larvicidal activites of ligand and its metal complexes have also been studied. The DNA cleavage activity of the ligand and its metal complexes have been studied.The result found that the Cu(II) complex effectively cleave pUC 18 DNA.

Key words:
Pyrrole-2-carboxaldehyde, Glutamic acid, XRD, SEM.

1. INTRODUCTION:

Heterocyclic compounds containing nitrogen, oxygen and sulphur have considerably a lot of attention due to wide application of pharmacological activity. Nitrogen, oxygen and sulfur are considered the most hetero atoms known[1]. In recent years, the coordination of Schiff bases to transition metal ions has been extensively
studied in medicine and diagnostics [2]. The substituted heterocyclic moiety in combination with transition metal salts generate coordination compounds which possess enhanced physiochemical and pharmacological properties [3–6]. Schiff base metal complexes have found their applications as catalysts in a wide range of reactions, such as polymerisation, epoxidation of olefins, ring-opening polymerisation, carbonylation reactions and oxidation reactions [7–11]. In this paper the metal complexes of Cu(II), Co(II), Mn(II), Zn(II) and Ni(II) with the Schiff base derived from pyrrole-2-carboxaldehyde with glutamic acid have been synthesized. The ligand and the metal complexes have been characterized by IR UV, ESI-mass, powder XRD, SEM and EDAX. The ligand and their metal complexes have been screened for their antimicrobial activities using the well diffusion method against the selected bacteria and fungai.

2. EXPERIMENTAL:

2.1 Material and Methods:

All reagents were analytical grade producers (Aldrich) and used without further purification. Chemical analysis of Carbon, Hydrogen and Nitrogen was performed using a Elemental vario EL III CHN analyzer.IR spectra of the ligand and complexes were recorded in the range of 4000-400cm^{-1} on JASCO FTIR-4100 Infrared spectrophotometer by KBR disc technique. UV-visible spectra was recorded using spectrophotometer with DMSO as the solvent in the range of 200-700 nm. ^{1}H NMR spectra were recorded in DMSO–d6 on a Bruker Avance 111,400 MHZ Spectrometer. X-ray diffraction study of some metal complexes were obtained on Rigaka D-Max C-Xray diffractometer. Scanning Electron microscope images were recorded in JEOL model JSM - 6390V electron microscopy.

2.2 Synthesis of Schiff base ligand potassium(S,Z)-2-(((1H-pyrrol-2-yl)methylene)amino)-4-Carboxy butanoate:

Pyrrole-2-carboxaldehyde (0.01 mol) is dissolved in 20 ml MeOH and added 20 ml methonic solution of Glutamic acid (0.01 mol) containing KOH (0.01 mol). The solution obtained was heated at 60° for 9 hours. Brownish yellow solution was formed. The volume of the solution is reduced to half. Filtered the precipitate, washed with ether followed by ethanol and dried in desiccators [12].

2.3 Synthesis of Schiff base metal complexes:

To the hot methanolic solution of Schiff base ligand (0.01 mol), and the methanolic solution of metal ions ($CoCl_2.6H_2O$, $CuCl_2.2H_2O$, $NiCl_2.2H_2O$, $MnCl_2.2H_2O$, $ZnCl_2$) was added drop by drop at 60° in 1:2 (metal:ligand) molar ratio. The mixture was then refluxed for 1 hour the intensity of the colour becomes translucent. The resulting mixture was filtered out, washed repeatedly with ether and dried in desiccator.

2.4 Antimicrobial activity:

2.4.1. Test organisms:

Bacterial species Bacillus subtilis, Bacillus cereus, Escherichia coli, Klebsiella pneumoniae, Pseudomonos aeruginosa, Staphylococcus aureus and fungal species Candida albicans and Aspergillus niger were used as test organisms.The Schiff base ligand and its metal complexes were screened against bacterial species such as Bacillus subtilis, Bacillus cereus, Escherichia coli, Klebsiella pneumoniae, Pseudomonos aeruginosa, Staphylococcus aureus and fungal species like Candida albicans and Aspergillus niger in agar well diffusion method. The Solvent used for dissolving the synthesised compounds was DMSO.

2.4.2. Experimental methods:

Muller hinton agar medium (20ml) was poured into each petri plate, and plates were swabbed with 100 µl inoculated of the test microorganisms and kept for 15 minutes for adsorption . Using sterile cork borer of 8mm diameter, wells were bored into the seeded agar plates, and these were located with a 100µl solution of each compound in DMSO. All the plates were incubated 37° for 24 hrs .After incubation , the inhibition growth was analysed and the results were recorded.

2.5 Larvicidal activity

The larvicidal activity of the samples was assessed by standard method. For the bioassay in a container 20 number of fourth instar larvae of *Culex quinquefasciatus* were kept in 49.9 ml of tap water with 0.1 ml of samples in DMSO. Larvae were fed a diet of rice bran extract. The Erlenmeyer flask containing the control larvae received 0.1 ml of DMSO served as negative control. After 24 h, 48 h and 72 h exposures the dead larvae were counted and the percentage mortality was recorded.

2.6 DNA cleavage:

Agarose gel electrophoresis

Agarose gel electrophoresis is a method for separating and visualizing DNA fragments. The fragments are separated by charge and size and movement through agarose gel matrix, when subjected to an electric field. The electric field is generated by applying potential across an electrolyte solution (buffer). When boiled in an aqueous buffer, agar dissolve and upon cooling solidifies to a gel. 1.5% agarose gel was prepared in 1x TE buffer and melted in hot water bath at 90 ˚C. Then the melted agarose was cooled down to 45 ˚C. 6 µl of 10 mg/ml of ethidium bromide was added and poured in to gel casting apparatus with the gel comb. After setting, the comb was removed from the gel. The electrophoresis buffer was poured in the gel tank and the platform with the gel was placed in it so as to immerse the gel. The gel was loaded with the samples and run at 50 V for 30 minutes. The stained gel was visualized using a gel documentation system (E gel imager, Invitrogen).

3. RESULTS AND DISCUSSION:

The analytical data and some physical properties of the ligand and its metal complexes are noted in table 1.The data shows that the complexes are formed in the ratio 1:2 (M : L). The resulting metal complexes were found to be stable at room temperature and insoluble in common solvents such as EtOH, MeOH but soluble in DMF and DMSO.

Table. 1 Analytical data and some physical properties of the ligand and metal complexes

Compound	Empirical Formula	Analytical data %				Molar Conductance (Ω^{-1} cm^2 mol^{-1}) DMSO	Colour	Mel. point
		Carbon	Hydrogen	Nitrogen	Metal			
PPMAP	$C_{10}H_{10}K_2N_2O_2$	39.98(C) 39.89 (A)	3.36(C) 3.23 (A)	9.33 (C) 9.31 (A)	-	-	Brown	140
$[Cu(PPMAP)_2]$	$C_{20}H_{20}CuN_4O_8$	47.29 (C) 47.23 (A)	3.97 (C) 3.50 (A)	11.03 (C) 11.00 (A)	12.51 (C) 12.35 (A)	5.41	Blue	146
$[Co(PPMAP)_2]$	$C_{20}H_{20}CoN_4O_8$	47.73(C) 47.38 (A)	4.01 (C) 4.53 (A)	11.13 (C) 11.08 (A)	11.71 (C) 11.60 (A)	15.63	Pink	185
$[Mn(PPMAP)_2]$	$C_{20}H_{20}MnN_4O_8$	48.11 (C) 48.51 (A)	4.04 (C) 4.42 (A)	11.22 (C) 11.28 (A)	11.00 (C) 11.36 (A)	10.06	Dirty White	150
$[Zn(PPMAP)_2]$	$C_{20}H_{20}ZnN_4O_8$	47.17 (C) 47.26 (A)	3.95 (C) 3.68 (A)	10.99 (C) 10.96 (A)	12.83 (C) 12.66 (A)	19.59	Dirty White	157
$[Ni(PPMAP)_2]$	$C_{20}H_{20}NiN_4O_8$	47.75 (C) 47.40 (A)	4.01 (C) 4.54(A)	11.14 (C) 11.08 (A)	11.67 (C) 11.56 (A)	16.78	Green	172

3.1 UV - Visible spectrum:

UV-Visible spectral data of the ligand and its complexes are presented in Table 2 and the spectrum of the ligand and Copper (II) complex is given in figure1, 2. The electronic spectra of the complexes were recorded from freshly prepared solution of DMSO at room temperature. The electronic spectrum of Schiff base ligand there are two absorption bands at 290, 447 nm assigned to $\pi - \pi*$ and $n - \pi*$ transitiitions. These transitions are also found in the spectra of the complexes, but they are shifted towards longer wavelength from ligand to complex, indicating coordination of ligand to metals through the azomethine moiety. The electronic spectrum showed the band absorption in the range 350, 490, 603 nm is assigned to $^2B_{1g} \rightarrow {}^2A_{1g}$, $^2B_{1g} \rightarrow {}^2B_{2g}$ and $^2B_{1g} \rightarrow {}^2E_g$ transition. These values suggested octahedral geometry. It has been further confirmed by the magnetic moment of Cu(II) complex is 1.98 B.M expected for one unpaired electron and it supports an octahedral geometry [13]. The Co(II) complex contains a d-d band at 743 nm, which corresponds to $^4A_{2g} \rightarrow {}^4T_{1g}$ (P) transitions [14]. There is a charge transfer band at 298 nm. The magnetic moment of Co(II) complex is 4.84 BM. The spectrum of Mn(II) complex contains bands at 343, 510, 984 nm. Those absorption bands may be assigned to the $^6A1_g \rightarrow {}^4A_1g$, $^6A1_g \rightarrow {}^4A_{2g}$, $A1_g \rightarrow {}^4Eg$ respectively. These bands suggested that the complex possess an octahedral geometry. The magnetic moment of Mn(II) complex is 5.97 BM. Zn(II) complex shows the bands at 259, 330, 403 nm due to charge transfer transition and an octahedral geometry was suggested for this complex [15]. The Zn(II) complex is found to be diamagnetic as expected for d^{10}configuration. Ni(II) complex display three bands at 400, 433, 852 nm describe to $^3A_{2g}(F) \rightarrow {}^3T_{2g}(F)$, $^3A_{2g}(F) \rightarrow {}^3T_{1g}(F)$, $^3A_{2g}(F) \rightarrow {}^3T_{1g}(P)$ transitions respectively these bands indicate that the complex have also an octahedral geometry Ni(II) complex showed the magnetic moment value of 3.12 B.M , in the range of 2.8-3.5 B.M suggesting the octahedral structure[16].

Table. 2 Electronic transitions and magnetic moment of PPMAP and its metal complexes

Compound	Absorption (nm)	Band assignment	Geometry and magnetic moment
PPMAP	290, 447	π - π*, n - π*	-
$[Cu(PPMAP)_2]$	294, 350, 490, 603	π - π*, $^2B_{1g} \rightarrow {}^2A_{1g}$, $^2B_{1g} \rightarrow {}^2B_{2g}$, $^2B_{1g} \rightarrow {}^2E_g$	Distorted Octahedral, 1.98 BM
$[Co(PPMAP)_2]$	298 , 743	π - π*, $^4A_{2g} \rightarrow {}^4T_{1g}(P)$	Octahedral, 4.84 BM
$[Mn(PPMAP)_2]$	343, 510,984	$^6A1_g \rightarrow {}^4A1_g$, $^6A1g \rightarrow {}^4A2_g$, $A1_g \rightarrow {}^4E_g$	Octahedral, 5.97BM
$[Zn(PPMAP)_2]$	259, 330, 403	π - π*, n - π*, LMCT	Octahedral, Diamagnetic
$[Ni(PPMAP)_2]$	400, 433, 852	$^3A_{2g}(F) \rightarrow {}^3T_{2g}(F)$, $^3A_{2g}(F) \rightarrow {}^3T_{1g}(F)$, $^3A_{2g}(F) \rightarrow {}^3T_{1g}(P)$	Octahedral, 3.12 BM

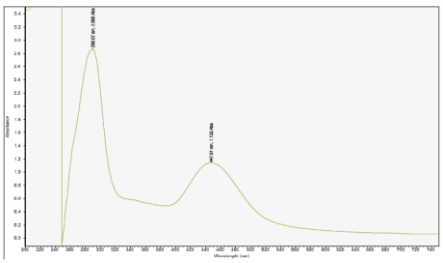

Figure 1 UV Spectrum of PPMAP

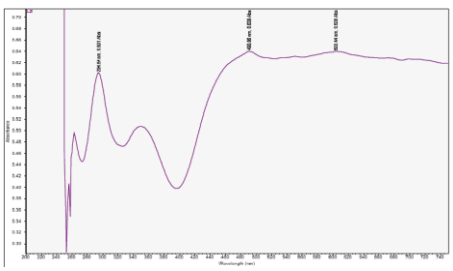

Figure 2 UV Spectrum of $[Cu(PPMAP)_2]$

3.2 IR Spectra:

Infrared spectral data of the ligand and its complexes are presented in Table.3 and the spectrum of the ligand and copper (II) complex are given in figure 3, 4. The band at 1680 cm^{-1} is due to azomethine group of the ligand undergoes a shift to lower frequency by about ~ 40 cm^{-1} in the IR spectra of the metal complexes. The shift of this group frequency in the spectra of the metal complexes suggested the coordination of azomethine nitrogen atom to metal ion [17]. The band at 1612 and 1440 cm^{-1} can be attributed to asymmetric carboxyl $V_{as}(COO^-)$ and symmetric carboxyl groups. During complexation these bands were shifted to lower frequency by ~20-30 cm^{-1} range indicating the linkage between the metal ion and carboxylato oxygen atom. The large difference between the $V_{as}(COO^-)$ and $V_s(COO^-)$ values of ~ 200 cm^{-1} indicates the monodentate binding nature of the carboxylato group in the complexes. A characteristic band at ~3200 cm^{-1}, due to (N-H) of pyrrole, was observed in the spectra of the ligand and their complexes. In the lower frequency region the weak bands observed at 525- 578 cm^{-1} and 400 - 486 cm^{-1} have been assigned respectively to the (M - O) and (M - N) vibrations [18]. Accordingly, it can be concluded that the ligand binds the metal ion in bidentate fashion. The bonding sites are the azomethine nitrogen and the carboxylato oxygen atoms.

Table. 3 IR spectral data of the PPMAP and its complexes (cm^{-1})

Compound	C = N	ν_s COO^-	ν_{as} COO^-	N-H	M-O	M-N
PPMAP	1680	1440	1612	3194	-	-
$[Cu(PPMAP)_2]$	1620	1396	1525	3198	540	486
$[Co(PPMAP)_2]$	1627	1411	1585	3200	540	400
$[Mn(PPMAP)_2]$	1643	1411	1550	3210	578	425
$[Zn(PPMAP)_2]$	1600	1411	1550	3210	525	410
$[Ni(PPMAP)_2]$	1643	1411	1581	3200	578	400

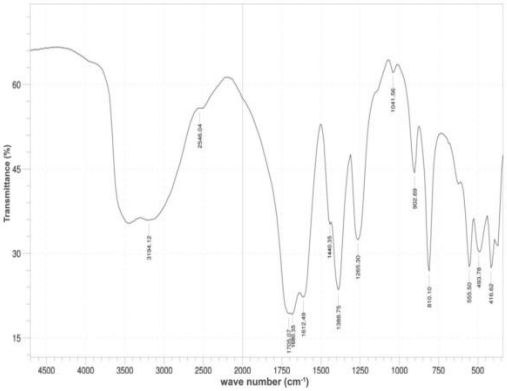

Figure 3 IR Spectrum of PPMAP

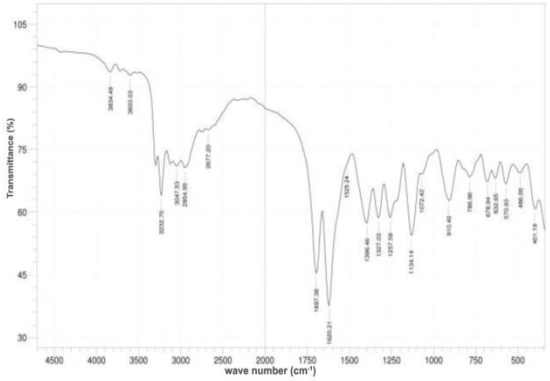

Figure 4 IR Spectrum of $[Cu(PPMAP)_2]$

3.3 ^{1}HNMR Spectra:

The ^{1}H NMR spectra of Schiff base ligand and the zinc(II) complex were recorded in DMSO - solution. Comparison of the ^{1}H NMR spectrum of the Schiff base with that of the corresponding Zinc(II) complex showed that some of the resonance signals experienced shifts upon the complexation.

The azomethine proton appeared as a sharp singlet at 8.28 ppm. Moreover, the azomethine proton of the free ligand is shifted down field to 9.47 ppm, indicating complexation of nitrogen atom of the azomethine with Zn(II). These observation suggest that the ligand coordinate with Zn(II) through the azomethine nitrogen and corboxylato oxygen atom. A new peak in the region 2.1 to 3.0 ppm characteristic of methylene group are present in the spectrum of the complex. The appearance of signals due to NH protons at the same positions in the ligand and its complex, show the non involvement of this group in coordination the peak value is 11.4 ppm [19]. The ^{1}H NMR spectrum of ligand and Zn(II) complex given by Figure 5,6.

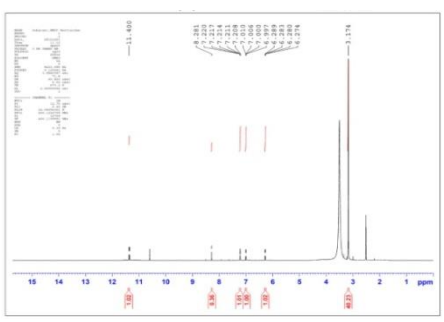

Figure 5 IR Spectrum of PPMAP

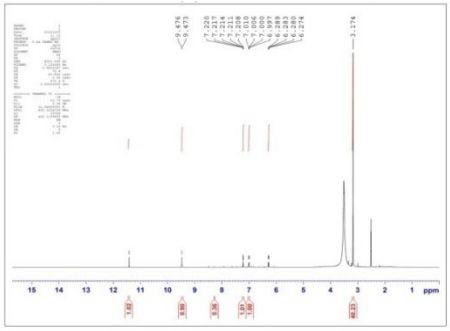

Figure 6 IR Spectrum of $[Cu(PPMAP)_2]$

3.4 EPR Spectra:

The X-band EPR spectra of Cu(II) complex were recorded in DMSO at liquid nitrogen temperature and at room temperature. The spectrum of Copper(II) complex was given Figure 7. The observed g|| and g⊥ values are 2.337 and 2.041 respectively. The g|| and g⊥ values are greater than 2.04, consistent with Copper (II) in axial symmetry with all the principal axes aligned parallel. These g values indicate an elongated tetragonally distorted octahedral stereochemistry [20]. From the values of g factors, it is calculate of the geometric parameter G, representing a measure of exchange interaction between Cu(II) centres in polycrystalline compound, using the formula.

$$G = g\| - 2.0023 / g\perp - 2.0023$$

If G < 4, it is considered the existence of some exchange interaction between Cu (II) centres and if G > 4, the exchange interaction is negligible. The present copper complex have G values greater than 4 indicating exchange interaction is either absent or very little in the solid complexes. The empirical ratio of g||/ A|| is frequently used to evaluate distortion in copper (II) complex. If the ratio is close to 100, it indicated roughly a square planer structure around the copper (II) ions and the values from 170 – 250 cm^{-1} are indicative of distorted tetrahedral geometry. If the ratio is between 110 and 170 cm^{-1}, it indicated nearly and octahedral environment around copper (II) ion with small distortion [21]. For the present copper complex the g|| /A|| value is 117cm^{-1} which indicate the complex have distorted octahedral geometry.

The covalency parameter α^2 and β^2 have been calculated using the following equations. If $\alpha^2 = 1.0$ it s indicated complete ionic character whereas $\alpha^2 = 0.5$ denotes 100% covalent bonding, with assumption of negligible small values of the overlap integral.

$$\alpha^2 = (A\|/0.036) + (g\| - 2.0027) + 3/7\ (g\perp - 2.0027) + 0.04$$

$$\beta^2 = (g\| - 2.0027)\ E / (-8\lambda\alpha^2)$$

In the present copper complex, the covalency parameter (α^2=0.50) indicates considerable covalent character for the metal ligand bond. Thus, the EPR study of the copper (II) complex has to provide supportive evidence to the conclusion obtained on the basis of electronic spectrum and magnetic moment value.

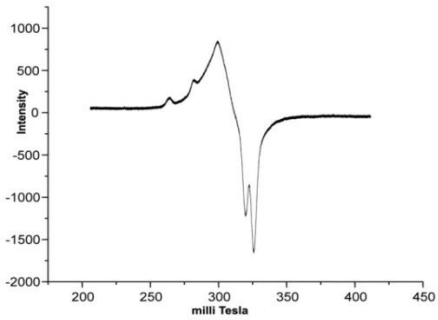

Figure 7 EPR Spectrum of $[Cu(PPMAP)_2]$

Based on the observations in elemental analysis IR, UV-Visible, ^{1}HNMR and EPR spectral studies, the proposed structure of Schiff base ligand and complexes. The Schiff base ligand and complexes are shown in Fig 8, 9.

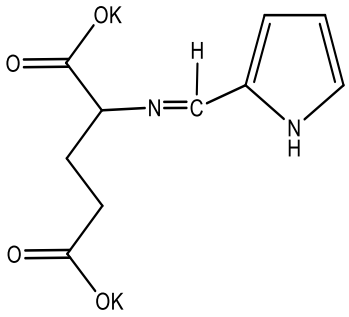

Figure 8 Structure of PPMAP

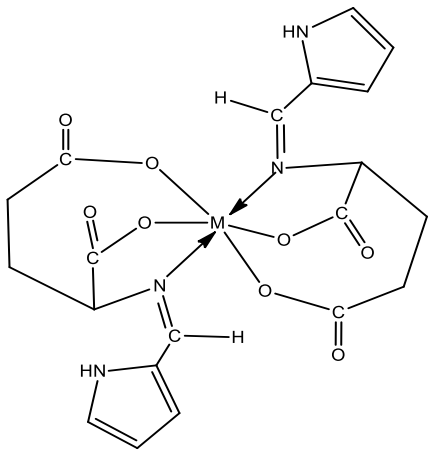

Figure 9 Structure of metal complexes Where M= Cu(II), Co(II), Mn(II), Zn(II) and Ni(II)

3.5 XRD:

The XRD pattern of ligand PPMAP figure 10 and $[Cu(PPMAP)_2]$ complex figure 11 shows well defined crystalline peaks indicating that the complex and the Schiff base ligand are crystallize in nature. The average crystalline size of the complexes d_{XRD} were calculated using Scherrer's formula [22].

$$d_{XRD} = 0.9\lambda/\beta \cos\theta$$

Where λ is the wavelength, β is the full-width half maximum of the characteristic peak and θ is the diffraction angle for the h k l plane. The average crystallize size of the ligand and the complex are 26.37 nm and 17.79 nm respectively suggesting that the ligand and complex are in a nanaocrystalline phase. The study also helped in characterizing the complex.

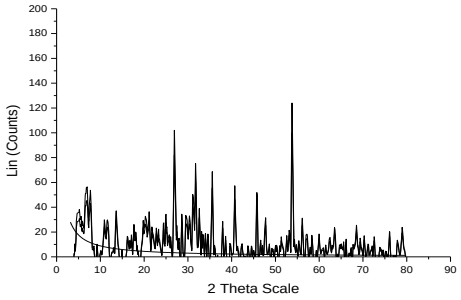

Figure 10 XRD spectrum of PPMAP

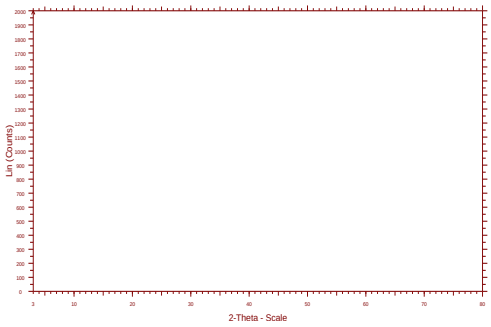

Figure11 XRD spectrum of $[Cu(PPMAP)_2]$

3.4 Scanning Electron Microscope (SEM):

The surface morphology of ligand is shown in Figure12. The SEM images of the Schiff base ligand have small ice cubes like morphology. This arrangements showed a thickness in the submicron regime. The surface morphology of Cu(II) complexes is shown in Figure13. The SEM images of the complex has flower like morphology. The size of the particle is less than 100 nm. The average crystallite size obtained from XRD also shows that the particles were agglomerated that these complexes have polycrystalline with nanosized grains [23].

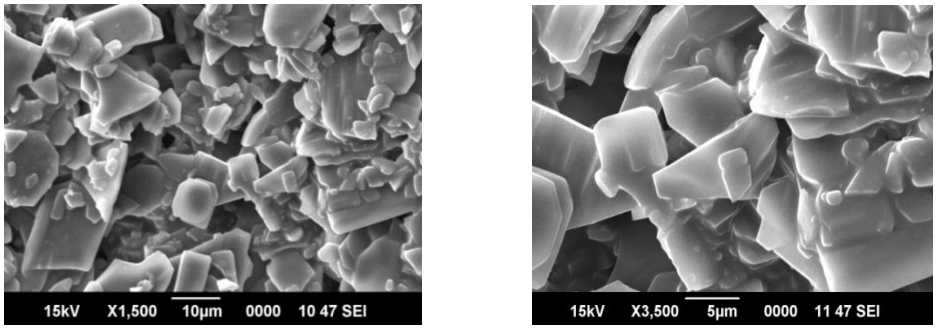

Figure 12 SEM Photograph of the PPMAP

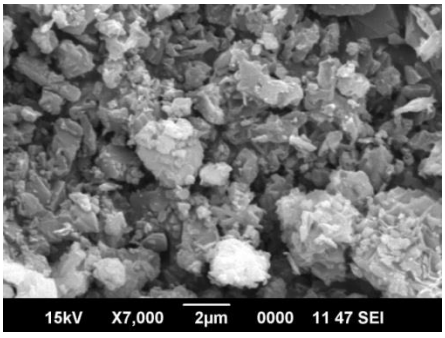

Figure 13 SEM Photograph of $[Cu(PPMAP)_2]$

3.5 EDAX Analysis:

EDAX can be used to determine which chemical elements present in the sample, and can be used to estimate their relative abundance. Elemental maping of a sample and image analysis are also possible as showed in Figure 14 and 15. The EDAX result of ligand showed that the atomic percentage of carbon, nitrogen, oxygen and potassium are 48.26, 6.18, 38.92 ,6.64% respectively while that of Cu(II) complex were found to be 46.85, 25.52, 12.47% for carbon, oxygen and copper respectively.

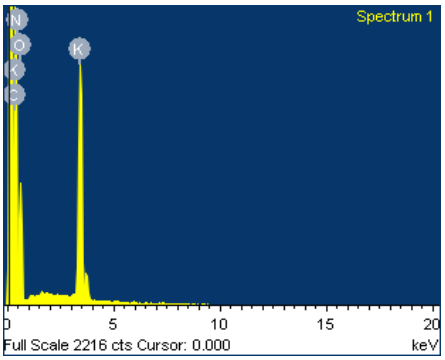

Figure 14 EDAX photograph of PPMAP

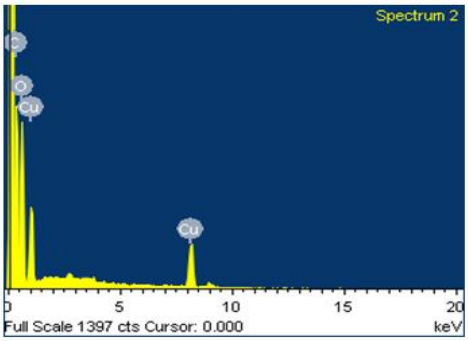

Figure 15 EDAX Photograph of [Cu(PPMAP)$_2$]

3.6 Antibacterial activity:

The ligand PPMAP, and its metal complexes were screened against six bacterial species such as B. Subtilis, B. Cereus, E.coli, K. Pneumonia, P. Aeruginosa, S. aureus to defect their anti bacterial properties. The results were presented in the Table 4 and Figure 16. The Cu (II) and Ni(II) complex have maximum inhibitory activity against *K. pneumoniae* and *P. aeruginosa*. Ni(II) complexes showed high activity against *E. coli* and the zone of inhibition was greater than the Schiff base ligand than the other complexes and the standard Amikacin. The Co(II) complex was found to be less active against all the bacterial species. Mn(II) and Zn(II) complexes were less active against *B. cereus* and *E. coli*. Zn(II) complex have moderate activity against *Staphylococcus aureus*. The Cu(II) complex showed highest activity against *E. coli*, *K. pneumoniae* and *Staphylococcus aureus* and the zone of inhibition was greater than the Schiff base ligand, other complexes and the standard Amikacin.

Table 4 Antibacterial activities of PPMAP and its metal complexes

	Zone of inhibition (mm)					
	B. subtilis	***B. cereus***	***E. coli***	***K. pneumoniae***	***P. aeruginosa***	***S. aureus***
PPMAP	7	8	8	5	5	7
[Cu(PPMAP)$_2$]	19	18	16	22	21	20
[Co(PPMAP)$_2$]	15	5	5	5	5	10
[Mn(PPMAP)$_2$]	5	10	5	12	15	10
[Zn(PPMAP)$_2$]	10	5	5	15	16	17
[Ni(PPMAP)$_2$]	8	16	15	20	25	9
Amikacin	23	23	11	20	27	20

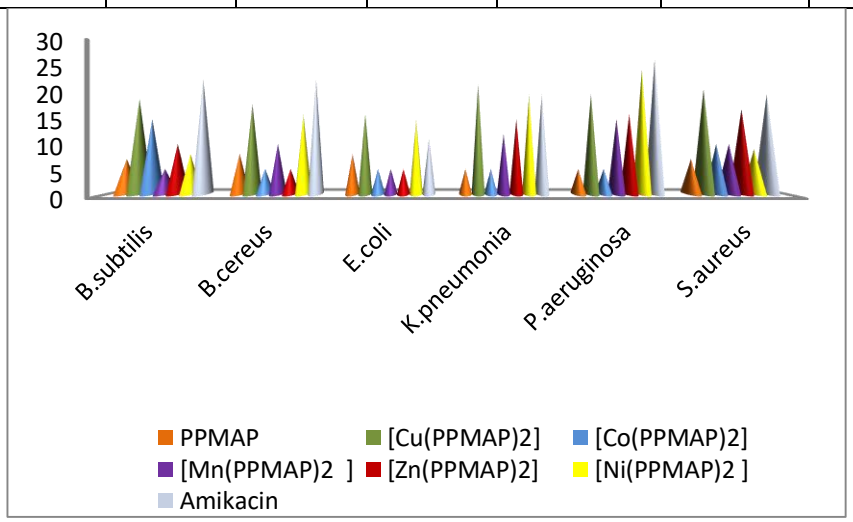

Figure 16 Anti bacteriogram of PPMAP and its metal complexes

3.7 Antifungal activity:

The results showed that the ligand PPMAP have minimum antifungal activity (Table 5 and Figure17). Whereas Cu(II), Zn(II) and Ni(II) complexes showed activity against *C. albicans.* Cu(II) and Co(II) complexes have active against *Aspergillus niger*. Ni(II) complex indicated highest activity against *C. albicans* followed by ligand, cobalt(II), maganese(II), zinc(II) and copper(II) complex. Cu(II) complex showed highest activity against *Aspergillus niger* followed by ligand, and other metal complexes.

Table 5 Antifungal Activities of PPMAP and its Metal Complexes

Compounds	**Zone of inhibition (mm)**	
	C. albicans	***A. niger***
PPMAP	5	7
$[Cu(PPMAP)_2]$	13	15
$[Co(PPMAP)_2]$	5	10
$[Mn(PPMAP)_2]$	5	5
$[Zn(PPMAP)_2]$	10	5
$[Ni(PPMAP)_2]$	17	5
Nystatin	16	14

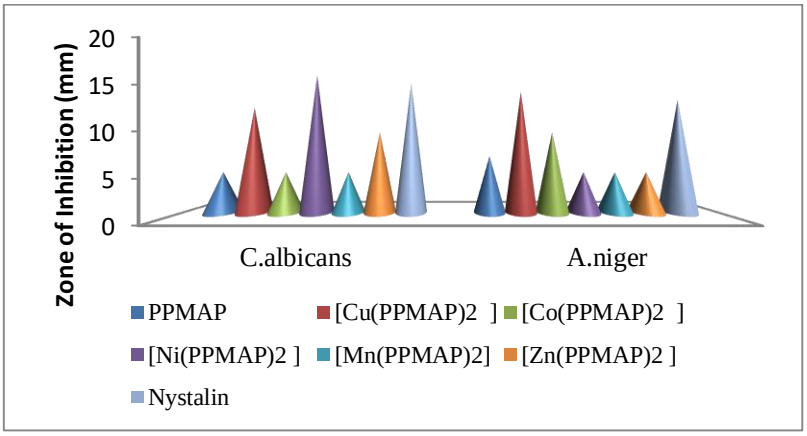

Figure 17 Antifungal spectrum of PPMAP and its metal complexes

It is found that metal complexes have higher antibacterial activity than the Schiff base ligand. Such increased activity of the metal complexes can be explained on the basis of overtone's concept and chelation theory[24,25]. On chelation the polarity of the metal ion will be reduced due to the overlapping of the ligand orbital and partial sharing of positive charge of the metal with donor groups. Itincreases the delocalization of -electrons over the whole chelate ring and enchances the lipoplicity of the complexes. This increased lipoplicity enchances the penetration of the complexes into lipid membranes and block the metal binding sites in the enzymes of microorganisms. The antimicrobial activity depends on the molecular structure of the compound, the solvent used and the species screened under consideration [26].

3.8 DNA cleavage:

In the present study, DNA cleavage experiment was performed using pUC18 plasmid DNA with ligand and complexes in the presence of H_2O_2. Photo induced DNA cleavage experiments have been carried out in UV light using the ligand PPMAP and the copper(II), cobalt(II), manganese(II), zinc(II) and nickel(II) complexes.

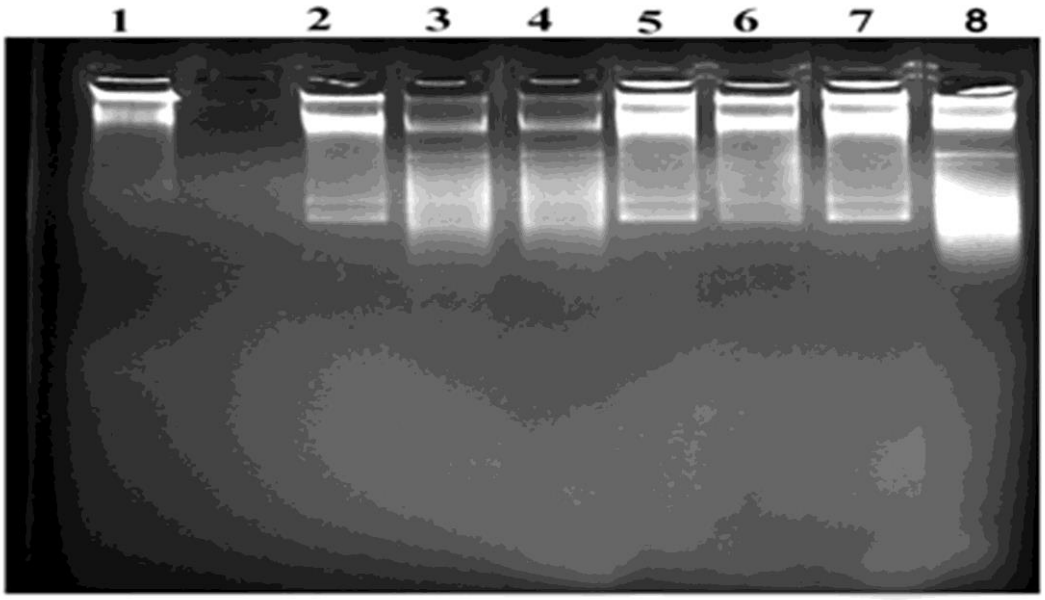

Figure 18 Gel electrophoresis for the DNA cleavage of PPMAP and its metal complexes

Lane 1: DNA control; Lane 2, DNA+PPMAP+ H_2O_2; Lane 3, DNA+ [$Cu(PPMAP)_2$] + H_2O_2; Lane 4, DNA+ [$Co(PPMAP)_2$] + H_2O_2; Lane5, DNA+ [$Mn(PPMAP)_2$] + H_2O_2; Lane6, DNA+ [$Zn(PPMAP)_2$] + H_2O_2; Lane7, DNA+ [$Ni(PPMAP)_2$] + H_2O_2; Lane 8, DNA+ H_2O_2

The results of the series of the ligand PPMAP and its metal complexes are shown in the Figure18 (Lane 1-8). From the result of this series of the ligand and its metal complexes it can be concluded that the copper(II) complex and cobalt(II) complex (lane 3,4) exhibits higher DNA cleavage activity. Zinc (II) complex also showed good DNA cleavage activity. Manganese(II) and nickel(II) complex showed moderate DNA cleavage activity.

3.9 Larvicidal Activity:

The larvicidal activity of the Schiff base ligand and the copper complex was performed against the larvae of culex and the result of mortality values are listed in table 6, 7. The pictorial representation of larvicidal activity is shown graph19.
LC50 value of copper complex = 30PPm
LC90 value of copper complex = 50PPm.
LC50 : Lethal concentration that kills 50 % of the exposed larvae
LC90 : Lethal concentration that kills 90 % of the exposed larvae
The metal complex showed enhanced larvicidal activity than the Schiffbase. The increased mortality rate observed for cu complex can be attriubuted to the increase in lippophilicity on complexation. Chelation increases the lipophilic nature of the central metal atom, which in turn, favours the molecules in crossing the cell membrane of the microorganism and enhancing larvicidal activity com

Table 6 Larvicidal activity of ligand and their Coper(II)complex

Compound	**Concentration ppm**	**Mortality rate of different time intervals**		
		24	48	72
PPMAP	1000	45	50	50
[$Cu(PPMAP)_2$]	1000	80	80	80

Table 7 Larvicidal activity of $[Cu(PPMAP)_2]$complex in various concentration

Compound	Concentration (ppm)	Mortality rate at different time intervals (h)					
		12	24	36	48	60	72
$[Cu(PPMAP)_2]$	20	5	15	30	50	80	90
	40	30	85	100	100	100	100
	60	65	90	100	100	100	100
	80	75	100	100	100	100	100
	100	85	100	100	100	100	100

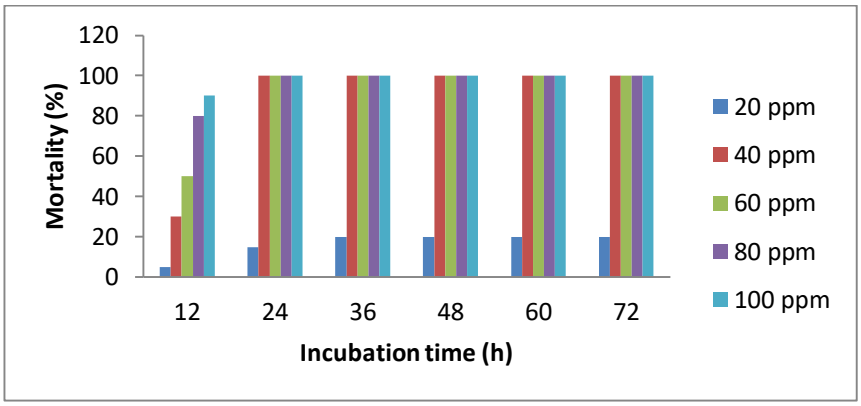

Figure 9. 40 Graph for Larvicidal activity of $[Cu(PPMAP)_2]$complex

4. CONCLUSION:

The Schiff base ligand PPMAP and it's (Cu), (Co), (Mn), (Zn) and (Ni) complexes were synthesized. The synthesized complexes were characterised by IR, UV, ^{1}HNMR, XRD, SEM and EDAX. They were tested for Antibacterial, Antifungal, Larvicidal and DNA cleavage activity. IR spectral data shows that the ligand act as bidentate, coordinating through azomethine nitrogen and carboxylato oxygen atoms. Electronic spectral studies revealed that Octahederal geometry for Cu(II), Co(II), Mn(II), Zn(II) and Ni(II) complexes. The XRD and SEM analysis explains the crystalline and morphological structure of the ligand and complexes. EDAX studies gave information about metal and elemental composition.The antimicrobial studies showed that the Schiff base ligand possesses mild activity and metal (II) complexes possesses higher activities against different bacterial and fungal strains. DNA cleavage studies found that the Cu(II) and Co(II) complex effectively cleave pUC 18 DNA. The larvicidal activitiy of the Schiff base and their Cu(II) complex have been also studied. The results revealed that the Cu(II) complex are showing more activity than the free ligand

5. ACKNOWLEDGEMENT

The authors acknowledge the department of chemistry and reaserch Nesamony Memorial Christian College, Marthandam, K.K. Dist for the facilities provided, STIC, Cochin - 22 for recording the various spectra and Biogenix Trivandrum for analyzing biological activities.

REFERENCES

1. Abu –Dief, AM. & Nassr, LAE. 2015.Tailoring, physicochemical characterization, antibacterial and DNA binding mode studies of Cu(II) Schiff base amino acid bioactive agents incorporating 5-bromo- 2- hyroxybenzaldehyde, Journal of Iranian Chemical Society. 12: 943-956.

2. Chang, H. Jia, L. Xu, J. Zhu, T. Xu, Z. Chen, R. Ma, T. Wang, Y. Wu, W. 2016. Syntheses, crystal structures, anticancer activities of three reduce Schiff base ligand based transition metal complexes. J. Mol. Struct. 1106: 366–372.

3. Inam, A. Siddiqui, S.M. Macedo, T.S. Moreira, D.R.M. Leite, A.C.L. Soares, M.B.P. Azam, A. 2014. Design, synthesis and biological evaluation of 3-[4-(7-chloro-quinolin-4-yl)-piperazin-1-yl]-propionic acid hydrazones as antiprotozoal agents. Eur. J. Med. Chem. 75: 67–76.

4. Júnior, W.B. Alexandre-Moreira, M.S. Alves, M.A. Perez-Rebolledo, A. Parrilha, G.L. Castellano, E.E. Piro, O.E. Barreiro, E.J. Lima, L.M. Beraldo, H. 2011. Analgesic and anti-inflammatory activities of salicylaldehyde 2-chlorobenzoyl hydrazone (H2LASSBio-466), salicylaldehyde 4-chlorobenzoyl hydrazone (H2LASSBio-1064) and their zinc(II) complexes. Molecules . 16: 6902–6915.

5. Muregi, F.W. Ishih, A.2010. Next-generation antimalarial drugs: Hybrid molecules as a new strategy in drug design. Drug Dev. Res. 71: 20–32.
6. Mohamed, G.G. Zayed, E.M. Hindy, A.M. 2015. Coordination behavior of new bis Schiff base ligand derived from 2-furan carboxaldehyde and propane-1,3-diamine. Spectroscopic, thermal, anticancer and antibacterial activity studies. Spectrochim. Acta Part A. 145: 76–84.
7. Seitz, M. & Alt H. G. 2006. Transition metal complexes of polymeric Schiff bases as catalyst precursors for the polymerization of ethylene. J. Mol. Catal. A Chem., 257: (1–2), 73–77.
8. Kuźniarska-Biernacka, I. et al. 2011. Epoxidation of olefins catalyzed by manganese(III) salen complexes grafted to porous heterostructured clays. Appl. Clay Sci., 53(2): 195–203.
9. Yao, L. et al. 2012. Ring opening polymerization of l-lactide by an electron-rich Schiff base zinc complex: An activity and kinetic study. J. Mol. Catal. A Chem., 352: 57–62.
10. Li-Juana, C., Mei, F.-M. & Guang-Xing, L. (2009). Co(II) Schiff base complexes on silica by sol–gel method as heterogeneous catalysts for oxidative carbonylation of aniline. Catal. Commun., 10: 981–985.
11. Gupta, K. C., Kumar Sutar, A. & Lin, C-C. (2009). Polymer-supported Schiff base complexes in oxidation reactions. Coord. Chem. Rev., 253(13–14): 1926–1946.
12. Arish, D & Sivasankaran Nair, M 2012, 'Synthesis characterization and biological studies of Co(II), Ni(II) and Zn(II) complexes with pyrral-L-histidinate', Arabian Journal of Chemistry, vol. 5, pp. 179-186.
13. Chandra, S 2009, 'Biological and spectral studies of transition metal complexes with a quinquedentate Schiff base, 2,6-diacetylpyridine bis(thiocarbohydrazone', Journal of Coordination Chemistry, vol. 62, pp.1327.
14. Geary, WJ 1971, 'The use of conductivity measurements in organic solvent for the characterization of coordination compounds', Coordination of Chemical Reviews, vol. 7, pp. 81-122.
15. Sekerci, M & Tas, E 2000, 'The synthesis and characterization of 1, 2-*O*-cyclohexylidene -4-aza-8-amino octane and some of its transition metal complexes', Heteroatom Chemistry, vol. 11, pp. 254-260.
16. Carlin, RN, Dryneveledt &Van AJ 1997, 'Magnetic Properties of Transition Metal Compounds Springer Verlag', New York.
17. Cukurovali, A, Yilmaz, I, Ozmen, H & Ahmedzade, M 2002, 'Schiff base ligands containing cyclobutane and their metal complexes with Co(II),Cu(II), Ni(II) and Zn(II) complexes of two novel Schiff base ligands and their antimicrobial activity', Transition Metal Chemistry, vol.27 , pp. 171-1761
18. Shebl, M 2009, 'Synthesis, spectral studies, and antimicrobial activity of binary and ternary Cu(II), Ni(II), and Fe(III) complexes of new hexadentate Schiff bases derived from 4,6-diacetyl resorcinol and amino acids', Journal of Coordination Chemistry, vol. 62, no.19, pp. 3217–3231.
19. Bhowon, MG, Li Kam Wah, H, Dosieah, A, Ridana, M, Ramalingum, O & Lacour, D 2004, 'Synhesis characterization and catalytic Activity of Metal Schiff base complexes Derived from pyrrole -2-Carboxaldehyde', Synthesis and Reactivity in Inorganic and Metal-organic chemistry, vol. 34, no. 1, pp. 1-16.
20. Singh, VP & Katiyar, A 2008, 'Synthesis, structural characterization and antimicrobial activity of some transition metal (II) complexes with acetone *p*-amino acetophenone benzoylhydrazone', Pesticide Biochemical Physiology, vol. 92, pp.8–14.
21. Hathaway, BJ & Billing, DE 1970, 'The electronic properties and stereochemistry of mono-nuclear complexes of the copper (II) ion', Coordination Chemical Reviews, vol. 5, no. 2, pp. 143–207.
22. Dhanaraj, CJ & Nair, MS 2009, 'Synthesis and characterization of metal (II) complexes of poly (3-nitro benzylidene-1-naphthylamine-*co*-succinic anhydride)', Europian Polymer Journal, vol. 45, no. 2, pp. 565-572.
23. Joseyphus, RS & Nair, M 2010, 'Synthesis, characterization and biological studies of some Co(II), Ni(II) and Cu(II) complexes derived from indole-3-carboxaldehyde and glycylglycine as Schiff base ligand', Arabian Journal of Chemistry, vol. 3, pp. 195–204.
24. Thimmaiah, K.N. Lloyd, W.D and Chandrappa G.T.1985. Extractive Spectrophotometric determination of molybdenum (V) in molybdenum steels. Inorg Chim Acta, 81:106.
25. Tweedy, B.G. 1964. Plant extracts with metal ions as potential antimicrobial agents, phytopathology, 55: 910- 914.
26. Jigna Parekh, 2005. Synthesis and antibacterial activity of some Schiff bases derived from 4-aminobenzoic acid. Serb. Chem. Soc, 70(10): 1155-1161.